Energy dependence of resonance production in relativistic heavy ion collisions*

Feng-Lan Shao(邵凤兰)[1;1)] Jun Song(宋军)[2] Rui-Qin Wang(王瑞芹)[1] Mao-Sheng Zhang(张茂盛)[1]

[1] School of Physics and Engineering, Qufu Normal University, Shandong 273165, China
[2] Department of Physics, Jining University, Shandong 273155, China

Abstract: The production of the hadronic resonances $K^{*0}(892)$, $\phi(1020)$, $\Sigma^*(1385)$, and $\Xi^*(1530)$ in central AA collisions at $\sqrt{s_{\rm NN}} = 17.3$, 200, and 2760 GeV is systematically studied. The direct production of these resonances at system hadronization is described by the quark combination model and the effects of hadron multiple-scattering stage are dealt with by a ultra-relativistic quantum molecular dynamics model (UrQMD). We study the contribution of these two production sources to final observation and compare the final spectra with the available experimental data. The $p_{\rm T}$ spectra of $K^{*0}(892)$ calculated directly by quark combination model are explicitly higher than the data at low $p_{\rm T} \lesssim 1.5$ GeV, and taking into account the modification of rescattering effects, the resulting final spectra well agree with the data at all three collision energies. The rescattering effect on $\phi(1020)$ production is weak and including it can slightly improve our description at low $p_{\rm T}$ on the basis of overall agreement with the data. We also predict the $p_{\rm T}$ spectra of $\Sigma^*(1385)$ and $\Xi^*(1530)$, to be tested by the future experimental data.

Keywords: resonance production, quark combination, relativistic heavy ion collisions

PACS: 25.75.Gz, 25.75.Nq **DOI:** 10.1088/1674-1137/41/1/014101

1 Introduction

Collisions of heavy ions at extremely relativistic energies create bulk matter with extremely high temperature and energy density [1]. The created matter expands, cools and finally produces thousands of hadrons of different species after hadronization. Compared to the stable hadrons, the produced hadronic resonances are significantly affected by the subsequent hadron multiple-scattering process, because of their short lifetime (usually several fm/c), which is less than or comparable to the time span of the hadronic stage. Resonances such as $K^{*0}(892)$, $\phi(1020)$ and $\Sigma^*(1385)$ have been measured by NA49 experiments at SPS energies, STAR experiments at RHIC energies and recent ALICE experiments at LHC energies, and rich experimental data of yields and transverse momentum $p_{\rm T}$ spectra are reported [2–6]. Their production has been studied by several models or event generators such as UrQMD, AMPT and hybrid methods [7–13].

In this paper, we study the production of these hadronic resonances in relativistic heavy ion collisions by focusing on both the initial production dynamics at hadronization and the effects of the hadronic rescattering stage. We choose three different collision systems, i.e., central Pb+Pb collisions at $\sqrt{s_{\rm NN}} = 17.3$ GeV, central Au+Au collisions at 200 GeV and central Pb+Pb collisions at 2760 GeV, which covers two order of the magnitudes of collision energy. This enables us to study the universal characteristics of resonance production in relativistic heavy ion collisions, taking advantage of the available data measured at SPS, RHIC and LHC. In particular, we discuss the initial production dynamics of hadronic resonances at hadronization. This is partially due to the microscopic production dynamics of stable hadrons such as pions, kaons, protons, Λ, Ξ and Ω being well established by the experimental data. It is the quark combination mechanism that microscopically dominates their production, not the traditional string fragmentation[2)]. Studying how these resonances are produced will deepen our understanding of the hadronization dynamics and test the existing hadronization models, which have been tested against the experimental data of stable hadrons, in relativistic heavy ion collisions. In order to present our results clearly, we adopt a two-step strategy. First, we use a combination model

Received 19 August 2016, Revised 23 September 2016

∗ Supported by National Natural Science Foundation of China (11575100, 11305076, 11505104)

1) E-mail: shaofl@mail.sdu.edu.cn

2) Relativistic hydrodynamics and statistical model are also very popular for thermal hadron production in relativistic heavy ion collisions. They describe the macroscopic (thermodynamical) behavior of the transition of quark gluon matter to hadronic matter, which is not the microscopic dynamics of the formation of hadrons out of final state quarks and/or gluons we study here.

to give the $p_{\rm T}$ spectra of resonance hadrons just after hadronization. Second, including the rescattering effect by a hadron transport model to give the final spectra of the resonances, and presenting them against the experimental data. We discuss whether the method of quark combination + hadron rescatterings can hold the essential characteristics of resonance production in relativistic heavy ion collisions or not.

We mainly study four resonance hadrons, i.e. $\rm K^{*0}(892)$, $\Sigma^*(1385)$, $\phi(1020)$, and $\Xi^*(1530)$, which have different properties in their production. $\rm K^{*0}(892)$ has a proper lifetime of about 4 fm/c and thus will decay quickly once it is produced. Their decay products, kaons and pions, can scatter with neighboring particles and thus lose the memory of their mother. On the other hand, the pions and kaons also have a certain probability of colliding to regenerate the $\rm K^{*0}(892)$. In addition, using available experimental data, we can study the production suppression of the vector $\rm K^{*0}(892)$ in the quark combination model, relative to its low-lying partner kaon (497 MeV). The $\phi(1020)$ meson has a long lifetime of about 46 fm/c, which is longer than the effective time duration of the hadronic rescattering stage. The initially produced $\phi(1020)$ is hardly lost and $\phi(1020)$ can also be produced by two kaon coalescence, and thus might have a rescattering effect to a certain extent. $\Sigma^*(1385)$ is a baryon resonance, and apart from the different reaction cross sections, the kinetics of daughter rescattering and regeneration is also different from the $\rm K^*$s. Thereby, we can study the baryon meson difference of hadronic rescattering effects. $\Xi^{*0}(1530)$ is a multi-strangeness hyperon, which can be used (together with $\Sigma^*(1385)$) to test the initial production of the $J^P = (3/2)^+$ state relative to the $J^P = (1/2)^+$ ground state and also the interaction dynamics of hyperons with light hadrons.

The paper is organized as follows. First we briefly introduce the quark combination model and hadronic rescattering model used in this work. Then we show the rescattering effects for the production of the above resonances, followed by a detailed discussion. Finally we show the final $p_{\rm T}$ spectra of four resonances and compare them with available experimental data. A summary is given at the end.

2 Brief introduction of working models

The quark combination model provides a good and natural description of hadron production in the low and intermediate $p_{\rm T}$ region for QGP hadronization [14–18], where the traditional string fragmentation fails. In this paper, we apply the quark combination model developed by the Shandong group (SDQCM) [18] to give the momentum spectra of hadronic resonances. Of all the combination models "on the market", SDQCM is unique for its combination rule, which guarantees that mesons and baryons exhaust the probability of all the fates of the (anti-)quarks in a deconfined color-neutral system at hadronization. The main idea of the combination rule is to line up the(anti-) quarks in a one-dimensional order in phase space, e.g., in rapidity, and then let them combine into initial hadrons one by one according to this order [18]. Three (anti-)quarks or a quark-antiquark pair in the neighborhood form a (anti-)baryon or a meson, respectively. The exclusive nature of the model makes it convenient to predict $\rm K^{*0}(892)$ and other resonance production on the basis of the reproduction of the yields and momentum spectra of various stable hadrons. The model has been used to explain the experimental data of yield, rapidity and $p_{\rm T}$ spectra of various identified hadrons in relativistic heavy ion collisions at different energies [18–23]. In those previous works, we have studied production of stable hadrons including pions, kaons, protons, Λ, Ξ and Ω at three collision energies. Assuming the same combination dynamics as those stable hadrons, we can directly compute the $p_{\rm T}$ spectra of the above resonances, using the obtained momentum distributions of quarks just before hadronization.

We use the ultra-relativistic quantum molecular dynamics model (UrQMD) [24, 25] version 3.4 to calculate the effects of the hadronic rescattering stage on resonance production. The UrQMD model is a non-equilibrium transport approach and provides a good description of the phase-space evolution of hadron systems. The interactions of hadrons include binary elastic and $2 \to n$ inelastic scatterings, resonance creations and decays, string excitations, particle-antiparticle annihilations as well as strangeness exchange reactions. The cross sections and branching ratios for the corresponding interactions are taken from available experimental measurements, detailed balance relations and the additive quark model. The model allows convenient study of the full phase-space evolution of all hadrons and resonances in relativistic heavy-ion collisions. In this paper, we use the hybrid mode of the UrQMD and at the chemical freeze-out point we input our calculated resonance spectra for hadronization via the Monte Carlo sampling method and then start the hadronic rescattering process. By comparing the spectra of the initial resonances with those taking into account the effects of the hadronic rescattering stage, we can study the presentation of the two main production sources at the final state.

3 Results of hadronic rescattering effects

Figure 1 shows the mid-rapidity $p_{\rm T}$ spectra of $\rm K^{*0}(892)$, $\phi(1020)$, $\Sigma^*(1385)$, and $\Xi^*(1530)$ directly produced by hadronization and those including the effects of the hadronic rescattering stage in central Pb+Pb col-

lisions at $\sqrt{s_{\rm NN}}$ = 17.3 GeV. Here, $\Sigma^*(1385)$ refers to $\Sigma^{*0}(1385)+\Sigma^{*-}(1385)$ plus their anti-particles in order to compare with the available experimental data and obtain high statistics. $\Xi^*(1530)$ refers to $\Xi^{*0}(1530)+\Xi^{*-}(1530)$. We see that the hadronic rescattering stage causes an obvious suppression on low $p_{\rm T}$ spectra of $K^{*0}(892)$ mainly because of the so-called signal loss, that is to say, $K^{*0}(892)$ decay products (pion and kaon) re-scattered by neighboring hadrons. With the increasing transverse momentum this signal loss becomes weak due to the prolonged fly lifetime (Lorentz effect). On the other hand, the regeneration of $K^{*0}(892)$ by pion kaon coalescence would contribute to the yield density at intermediate $p_{\rm T}$, as seen in $p_{\rm T} \sim 2$ GeV in Fig. 1(a). We see that the spectrum of the $\phi(1020)$ meson is slightly affected by hadronic rescatterings. For $\Sigma^*(1385)$ and $\Xi^*(1530)$, hadronic rescatterings also suppress their low $p_{\rm T}$ spectra but the magnitude is smaller than that of $K^{*0}(892)$. It also causes a slight increase of the yield density at the moderate $p_{\rm T}$ region, which is the competition of signal loss and regeneration channels.

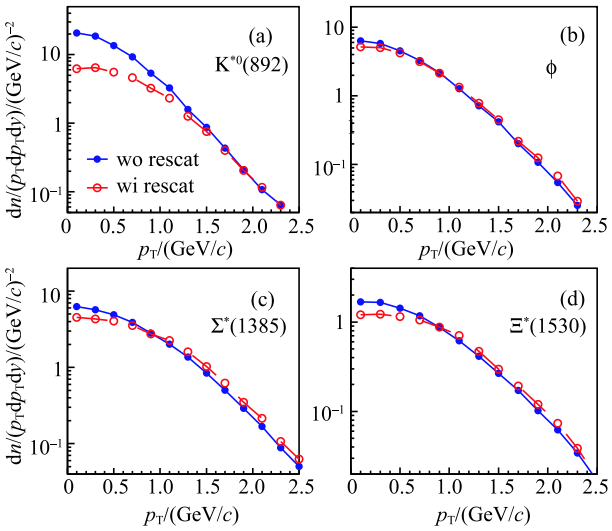

Fig. 1. (color online) Mid-rapidity $p_{\rm T}$ spectra of resonances with/without including the effects of the hadronic rescattering stage in central Pb+Pb collisions at $\sqrt{s_{\rm NN}}$ = 17.3 GeV.

The effects of the hadronic rescattering stage at different collision energies are shown in Fig. 2. Here, in order to study their energy dependence, we plot the ratio of $p_{\rm T}$ spectra of resonances incorporating the hadronic rescattering effects to those that don't. Figure 2(a) shows the results of $K^{*0}(892)$ in central AA collisions at $\sqrt{s_{\rm NN}}$ =17.3, 200 and 2760 GeV. We see that the production of $K^{*0}(892)$ is suppressed by more than half at low $p_{\rm T}$, and as $p_{\rm T}$ increases the suppression becomes weak due to the contribution of the regeneration channel. In addition, we see a weak energy dependence for the ratio of $K^{*0}(892)$ from 17.3 GeV to 200 GeV but an obvious continuous suppression as the collision energy increases to 2760 GeV, which is partially due to the much extended lifetime of the hadronic phase at LHC energies. For $\phi(1020)$ in Fig. 2(b), the ratio deviates from one by around 20% in the $p_{\rm T}$ region covered both at 17.3 GeV and 200 GeV, showing also a weak energy dependence from SPS to RHIC energies. At LHC energy, the $\phi(1020)$ suppression at the low $p_{\rm T}$ region is relatively strong and reaches about 30%. Compared to panel (a), the hadronic rescattering effect on the $\phi(1020)$ is obviously smaller than that of the $K^{*0}(892)$. This is closely related to the $\phi(1020)$'s long lifetime and the small reaction cross section between $\phi(1020)$ and other particles. Note that two kaon coalescence can regenerate $\phi(1020)$ and thus increase the $\phi(1020)$ yield at the intermediate $p_{\rm T}$ region to a certain extent (10%–20%), which is determined by their cross section and their phase space populations in the system evolution. For $\Sigma^*(1385)$ and $\Xi^*(1530)$, we also find a nontrivial suppression at the low $p_{\rm T}$ region and a small increase at moderate $p_{\rm T}$ due to the competition of signal loss and regeneration.

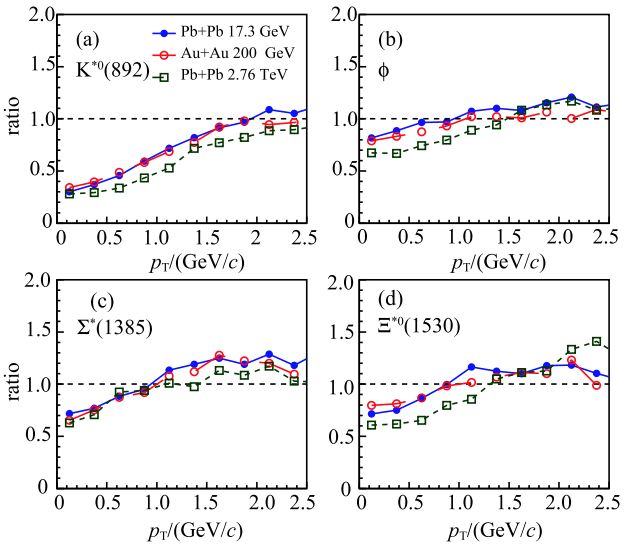

Fig. 2. (color online) The ratio of the $p_{\rm T}$ spectra of resonances incorporating hadronic rescattering effects to those without, at three different collision energies. The imperfect smoothness is due to the finite statistics.

4 Final spectra of resonances

In Fig. 3, we present the $p_{\rm T}$ spectra of initial and final $K^{*0}(892)$ taking into account rescattering effects at three different collision energies, and compare them with the experimental data [2, 4, 6]. The open circles with dashed lines are $p_{\rm T}$ spectra of direct $K^{*0}(892)$ given by SDQCM. We see that at the low $p_{\rm T}$ region $p_{\rm T} \lesssim 1$

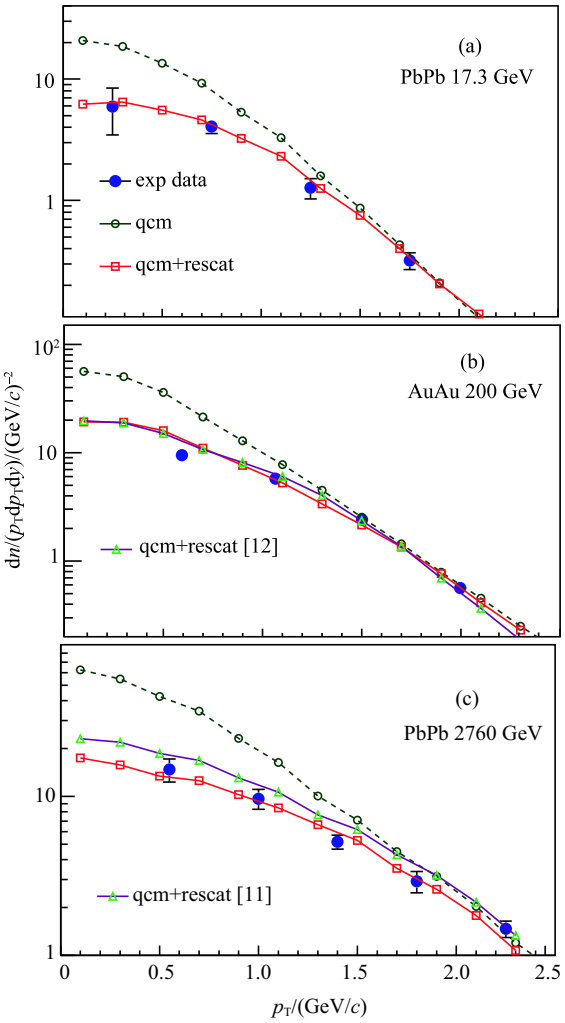

Fig. 3. (color online) The p_T spectra of $K^{*0}(892)$ at three different collision energies. Solid circles are experimental data [2, 4, 6] and open symbols with lines are results of initially produced $K^{*0}(892)$ by SDQCM and of those including hadron rescattering effects, respectively.

GeV, the $K^{*0}(892)$ produced by hadronization is obviously greater than the data at the three collision energies. As p_T increases, the QCM results begin to get closer to the data. Note that these direct spectra of $K^{*0}(892)$ are calculated using the momentum distribution of constituent light quarks and strange quarks obtained in previous works, where we have reproduced the experimental data of various stable hadrons, in particular, that of kaons. The over-estimation at low p_T shows the necessity of including the significant effects of the hadronic rescattering stage. Including these effects, we get the final spectra of $K^{*0}(892)$, which are shown as the open squares with solid lines in Fig. 3 (a-c). In panel (a), for Pb+Pb 17.3 GeV, we obtain a good description of experimental data. For panel (b), at Au+Au 200 GeV, we also get an improved agreement with the data. Here, we also plot another result, up-triangles with solid line, in which the hadronic rescattering effect is calculated from the ART subroutine in the AMPT model obtained in our previous work [12]. We find that it is very close to the present one. At LHC energy in panel (c), consideration of the hadronic rescattering effects significantly suppresses the low p_T $K^{*0}(892)$ production and the final p_T spectrum tends to agree with the experimental data of the ALICE collaboration [6]. Here, we also plot another result in which the hadronic rescattering effect is calculated in Ref. [11], and it can be regarded as a reference for the theoretical uncertainty of the hadronic stage. The final $K^{*0}(892)$ spectrum obtained is shown as the up-triangles with solid line in panel (c). This result exhibits weaker suppression than we calculated. It slightly exceeds the data in $p_T \lesssim 2$ GeV by about 20%, but agrees with the last data point. Together these two results, we argue that the experimental data can be explained by the method of this paper. The results of Fig. 3 thus give us significant confidence that the initial production dynamics of $K^{*0}(892)$ at hadronization should also be quark combination.

In meson formation in the quark combination model, the relative production probability of the lowest-lying vector meson (V) to pseudo-scalar meson (P) with the same constituent quark composition is tuned by the parameter $R_{V/P}$. In previous work [12] at high RHIC energies, we found that a value of about 0.45 for $R_{V/P}$ can explain the data of kaons and $K^{*0}(892)$ simultaneously. Here, we see that using the same value, the data of both SPS and LHC energies are also explained well. This universal parameter value suggests a nontrivial constraint for modeling the spin-induced interaction dynamics at hadronization in more sophisticated quark combination models in future.

Figure 4 shows the results for the $\phi(1020)$ meson and the comparison with experimental data [3, 6, 26]. As shown in Fig. 2, the rescattering effect of $\phi(1020)$ production is weak, which is due to its long lifetime and small interaction cross section with other particles, and relatively rare two kaon coalescence. The final $\phi(1020)$ p_T spectra including the rescattering effects, open-squares with solid line, change little relative to the initial ones given by SDQCM, open-circles with dashed lines. We find a good agreement with the experimental data at SPS (panel (a)) and RHIC (panel (b)). As the collision energy increases to LHC energy, see panel (c), the rescattering effects suppress, to a certain extent, the yield density of the $\phi(1020)$ meson at low $p_T(\lesssim 1$ GeV) and we observe an visible decrease for the final $\phi(1020)$ spectra there, leading to an improved agreement between our final result and the experimental data of the ALICE collaboration.

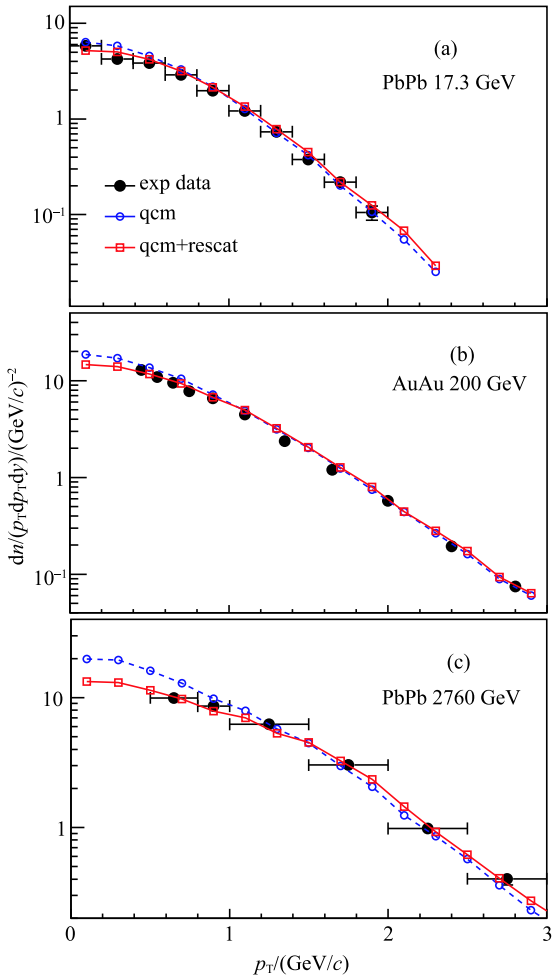

Fig. 4. (color online) The p_T spectra of $\phi(1020)$ at three different collision energies. Solid circles are experimental data [3, 6, 26] and open symbols with lines are results of initially produced $\phi(1020)$ by SDQCM and of those including hadron rescattering effects, respectively.

Some comments on $\phi(1020)$ results at LHC energies are in order. The data show the p_T spectrum of the proton is very close to that of $\phi(1020)$ [6], which is expected in the hydrodynamical model mainly due to their similar mass. So it is argued in Ref. [6] that the $\phi(1020)$ meson production is thermal dominated at LHC energies. Surely, thermalization is more important at LHC. However, we note that the shape of the $\phi(1020)$ distribution calculated by the hydrodynamical model still deviates from the data to a certain extent [6, 31], i.e. it overestimates the production by about 50% at $p_T \lesssim 2$ GeV but underestimates the data by almost the same proportion at larger p_T. In addition, the hydrodynamical model fails to reproduce the $\Omega/\phi(1020)$ ratio as a function of p_T as $p_T \gtrsim 2$ GeV [6]. Note that the exponential behavior of the hadronic p_T spectra at LHC extends to 4 GeV for mesons and 6 GeV for baryons due to the large collective flow [28]. On the other hand, at LHC energy QCM still performs as well as at RHIC energies, as shown in Fig. 4 for $\phi(1020)$ and our previous work [21] for stable hadrons. To illustrate it more clearly, Fig. 5 shows the p_T spectra of various stable strange hadrons obtain in our work [21] with further refined quark spectra for thermal components. The p_T region is chosen as 0–4 GeV, because we observe that the $\Omega/\phi(1020)$ ratio linearly increases to about 4 GeV [6], showing the dominant region for thermal quark combination. The relative difference between our results and the data is less than about 20%, which is smaller than those of the hydrodynamical model and others reported in the literature [6, 29, 31–35].

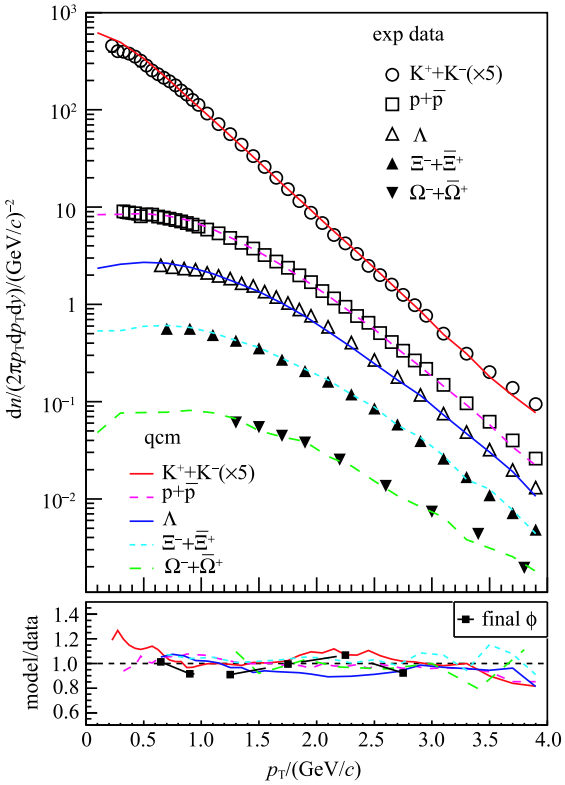

Fig. 5. (color online) The p_T spectra of stable hadrons in central Pb+Pb collisions at $\sqrt{s_{NN}} =$ 2760 GeV. Symbols are the experimental data [27–30] and lines are the results of SDQCM. The data and model results for the kaon are multiplied by a factor of 5 for clarity.

Finally, we show the results of the final $\Xi^*(1530)$ and $\Sigma^*(1385)$ in Fig. 6. In SDQCM, the relative production of the lowest-lying decuplet baryon ($J^P = (3/2)^+$) to octet baryon ($J^P = (1/2)^+$) with the same constituent quark composition is tuned by the parameter $R_{D/O}$, which is taken to be 0.5 based on symmetry analysis and the data of pp and e^+e^- collisions in our previous works [18]. At present, only the data of $\Sigma^*(1385)$ at

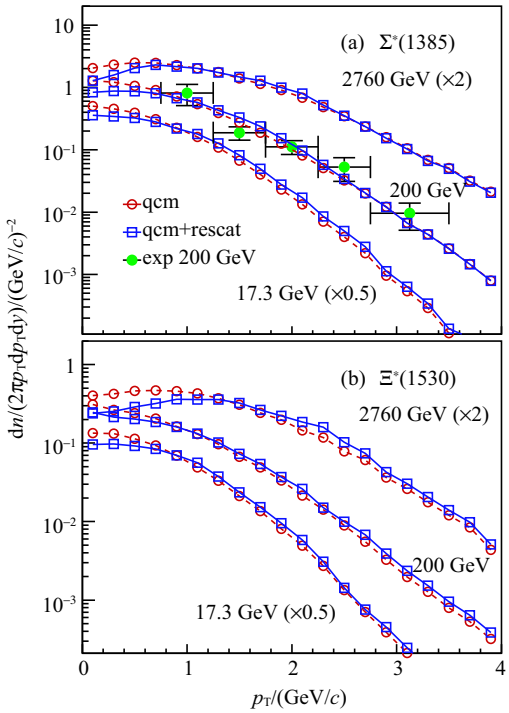

Fig. 6. (color online) The $p_{\rm T}$ spectra of $\Sigma^*(1385)$ and $\Xi^*(1530)$ with/without incorporation of hadronic rescattering effect, at three different collision energies.

Au+Au collisions are available and are shown also in panel (a). We see that our results at 200 GeV basically agree with the data. The results for SPS and LHC energies are left to be tested by future experimental data. For $\Xi^*(1530)$, the rescattering effects at LHC energy are stronger than that for $\Sigma^*(1385)$ but are still smaller than that for $\rm K^{*0}(892)$. We predict their final spectra for future testing by experimental data.

5 Summary

We have studied the production of the hadronic resonances $\rm K^{*0}(892)$, $\phi(1020)$, $\Sigma^*(1385)$, and $\Xi^*(1530)$ in relativistic heavy ion collisions, using the hybrid method of quark combination hadronization plus hadronic multiple scattering effects. The experimental data of $\rm K^{*0}(892)$ and $\phi(1020)$ at central Pb+Pb collisions at $\sqrt{s_{\rm NN}} = 17.3$, central Au+Au collisions at 200 GeV and central Pb+Pb collisions at 2760 GeV are explained well. We find that the effect of hadronic rescattering causes significant suppression of $\rm K^{*0}(892)$ production at low $p_{\rm T}$ but slight suppression for $\phi(1020)$ production. The effect of hadronic rescattering is also nontrivial for $\Sigma^*(1385)$ and $\Xi^*(1530)$ production. We predict the final $p_{\rm T}$ spectra of $\Sigma^*(1385)$ and $\Xi^*(1530)$ for future tests by experiments.

References

1 Quark Gluon Plasma 3, edited by R. C. Hwa and X. N. Wang (Singapore: World Scientific, 2004)
2 T. Anticic et al (NA49 Collaboration), Phys. Rev. C, **84**: 064909 (2011)
3 C. Alt et al (NA49 Collaboration), Phys. Rev. C, **78**: 044907 (2008)
4 M. M. Aggarwa et al (STAR Collaboration), Phys. Rev. C, **84**: 34909 (2011)
5 B. I. Abelev et al (STAR Collaboration), Phys. Rev. Lett., **97**: 132301 (2006)
6 B. B. Abelev et al (ALICE Collaboration), Phys. Rev. C, **91**: 024609 (2015)
7 M. Bleicher and J. Aichelin, Phys. Lett. B, **530**: 81 (2002)
8 M. Bleicher, Nucl. Phys. A, **715**: 85c (2003)
9 S. Vogel and M. Bleicher, arXiv: nuclth/0505027
10 S. Vogel, J. Aichelin, and M. Bleicher, J. Phys. G, **37**: 094046 (2010)
11 A. G. Knospe, C. Markert, K. Werner et al, Phys. Rev. C, **93**: 014911 (2016)
12 K. Zhang, J. Song, and F. L. Shao, Phys. Rev. C **86**: 014906 (2012)
13 K. C. Liu, J. Song, and F.L. Shao, Int. J. Mod. Phys. E, **23**: 1450060 (2014)
14 R. J. Fries, B. Müller, C. Nonaka et al, Phys. Rev. Lett., **90**: 202303 (2003)
15 V. Greco, C. M. Ko, and P. Lévai, Phys. Rev. Lett., **90**: 202302 (2003)
16 R. C. Hwa and C. B. Yang, Phys. Rev. C, **70**: 024905 (2004)
17 L. W. Chen and C. M. Ko, Phys. Rev. C, **73**: 044903 (2006)
18 F. L. Shao, Q. B. Xie, and Q. Wang, Phys. Rev. C, **71**: 044903 (2005); C. E. Shao, J. Song, F. L. Shao et al, Phys. Rev. C, **80**: 014909 (2009)
19 R. Q. Wang, F. L. Shao, J. Song et al, Phys. Rev. C, **86**: 054906 (2012)
20 J. Song and F. L. Shao, Phys. Rev. C, **88**: 027901 (2013)
21 R. Q. Wang, J. Song, and F. L. Shao, Phys. Rev. C, **91**: 014909 (2015)
22 L. X. Sun, R. Q. Wang, J. Song et al, Chin.Phys. C, **36**(1): 55 (2012)
23 J. Song, F. L. Shao, Q. B. Xie et al, Chin. Phys. C, **33**(6): 481 (2009)
24 S. A. Bass, M. Belkacem, M. Bleicher et al, Prog. Part. Nucl. Phys., **41**: 225 (1998)
25 M. Bleicher, E. Zabrodin, C. Spieles et al, J. Phys. G, **25**: 1859 (1999)
26 B. I. Abelev et al (STAR Collaboration), Phys. Rev. Lett., **99**: 112301 (2007)
27 B. B. Abelev et al (ALICE Collaboration), Phys. Rev. Lett., **109**: 252301 (2012)
28 B. B. Abelev et al (ALICE Collaboration), Phys. Lett. B, **736**: 196 (2014)
29 B. B. Abelev et al (ALICE Collaboration), Phys. Lett. B, **728**: 216 (2014)
30 B. B. Abelev et al (ALICE Collaboration), Phys. Rev. Lett., **111**: 222301 (2013)
31 C. Shen, U. Heinz, P. Huovinen et al, Phys. Rev. C, **84**: 044903 (2011)
32 Iu.A. Karpenko and Yu.M. Senyukov, J. Phys. G, **38**: 124059 (2011)
33 Iu.A. Karpenko, Yu.M. Sinyukov, and K. Werner Phys. Rev. C, **87**: 024914 (2013)
34 P. Bozek, Phys. Rev. C, **85**: 034901 (2012)
35 P. Bozek, Acta Phys. Pol. B, **43**(4): 689 (2012)